LETTERS

Direct observation of Anderson localization of matter waves in a controlled disorder

Juliette Billy[1], Vincent Josse[1], Zhanchun Zuo[1], Alain Bernard[1], Ben Hambrecht[1], Pierre Lugan[1], David Clément[1], Laurent Sanchez-Palencia[1], Philippe Bouyer[1] & Alain Aspect[1]

In 1958, Anderson predicted the localization[1] of electronic wavefunctions in disordered crystals and the resulting absence of diffusion. It is now recognized that Anderson localization is ubiquitous in wave physics[2] because it originates from the interference between multiple scattering paths. Experimentally, localization has been reported for light waves[3–7], microwaves[8,9], sound waves[10] and electron gases[11]. However, there has been no direct observation of exponential spatial localization of matter waves of any type. Here we observe exponential localization of a Bose–Einstein condensate released into a one-dimensional waveguide in the presence of a controlled disorder created by laser speckle[12]. We operate in a regime of pure Anderson localization, that is, with weak disorder—such that localization results from many quantum reflections of low amplitude—and an atomic density low enough to render interactions negligible. We directly image the atomic density profiles as a function of time, and find that weak disorder can stop the expansion and lead to the formation of a stationary, exponentially localized wavefunction—a direct signature of Anderson localization. We extract the localization length by fitting the exponential wings of the profiles, and compare it to theoretical calculations. The power spectrum of the one-dimensional speckle potentials has a high spatial frequency cutoff, causing exponential localization to occur only when the de Broglie wavelengths of the atoms in the expanding condensate are greater than an effective mobility edge corresponding to that cutoff. In the opposite case, we find that the density profiles decay algebraically, as predicted in ref. 13. The method presented here can be extended to localization of atomic quantum gases in higher dimensions, and with controlled interactions.

The transport of quantum particles in non-ideal material media (for example the conduction of electrons in an imperfect crystal) is strongly affected by scattering from the impurities in the medium. Even for weak disorder, semiclassical theories, such as those based on the Boltzmann equation for matter waves scattering from the impurities, often fail to describe transport properties[2], and fully quantum approaches are necessary. For example, Anderson localization[1], which predicts metal–insulator transitions, is based on interference between multiple scattering paths, leading to localized wavefunctions with exponentially decaying profiles. While Anderson's theory applies to non-interacting particles in static (quenched) disordered potentials[1], both thermal phonons and repulsive interparticle interactions significantly affect Anderson localization[14,15]. To our knowledge, no direct observation of exponentially localized wavefunctions in space has been reported in condensed matter.

Degenerate atomic quantum gases can be used to study a number of basic models in condensed matter theory experimentally, with unprecedented control and measurement possibilities (see refs 16, 17 and references therein). In investigating the behaviour of matter waves in disordered potentials[18], key advantages of atomic quantum gases are the possibility to implement systems in any dimension; the control of the interatomic interactions, either by density control or by Feshbach resonances; the possibility to design perfectly controlled and phonon-free disordered potentials; and the opportunity to measure *in situ* atomic density profiles via direct imaging. The quest for evidence of Anderson localization of Bose–Einstein condensates (BECs) in optical disordered potentials has thus attracted considerable attention in recent years[19–22]. Experiments using ultracold atoms have shown evidence of dynamical localization associated with a kicked rotor[23,24], which can be considered as a mapping onto momentum space of the Anderson localization phenomenon. Suppression of one-dimensional transport of BECs has been observed[19,20], but this occurred in a regime of strong disorder and strong interactions where localization is due to classical reflections from large peaks of the disordered potential. Here we report direct observation in real space of one-dimensional localization of a BEC in the regime of Anderson localization, that is, with weak disorder and negligible interatomic interactions.

Our experiment (sketched in Fig. 1a, b), starts with a small, elongated BEC (1.7×10^4 atoms of rubidium-87, with transverse and longitudinal radii of 3 μm and 35 μm, respectively, corresponding to the trapping frequencies given below, and a chemical potential of $\mu_{in}/h = 219$ Hz, where h is Planck's constant). The BEC is produced in an anisotropic opto-magnetic hybrid trap. A far-off-resonance laser beam (wavelength 1.06 μm, to be compared with the resonant wavelength of rubidium, 0.78 μm) creates an optical waveguide along the horizontal z axis[25], with a transverse harmonic confinement of frequency $\omega_\perp/2\pi = 70$ Hz. A shallow magnetic trap confines the BEC in the longitudinal direction ($\omega_z/2\pi = 5.4$ Hz).

The longitudinal confinement is switched off at $t = 0$, and the BEC starts to expand in the guide along the z direction under the effect of the initial repulsive interaction energy. A weakly anti-trapping magnetic field compensates the residual longitudinal trapping of the optical waveguide, so that the atoms can freely expand along the z direction over several millimetres. The expanding BEC can be imaged at any chosen time t after release by switching off the optical guide and irradiating the atoms with a resonant probe of duration 50 μs. An ultrasensitive electron-multiplying charge-coupled-device camera allows us to make an image of the fluorescing atoms with a resolution of 15 μm and a one-dimensional atomic density sensitivity of close to one atom per micrometre.

A disordered potential is applied to the expanding BEC using an optical speckle field produced by passing a laser beam (wavelength 0.514 μm) through a diffusing plate[22]. The detuning from the atomic frequency is great enough, and the intensity low enough, that spontaneous photon scattering on the atoms is negligible during the expansion, and we have a purely conservative disordered potential,

[1]Laboratoire Charles Fabry de l'Institut d'Optique, CNRS and Univ. Paris-Sud, Campus Polytechnique, RD 128, F-91127 Palaiseau cedex, France.

which extends 4 mm along the z direction. The three-dimensional autocorrelation of the disordered potential—that is, of the light intensity—is determined by diffraction from the diffusive plate onto the atoms' location[22].

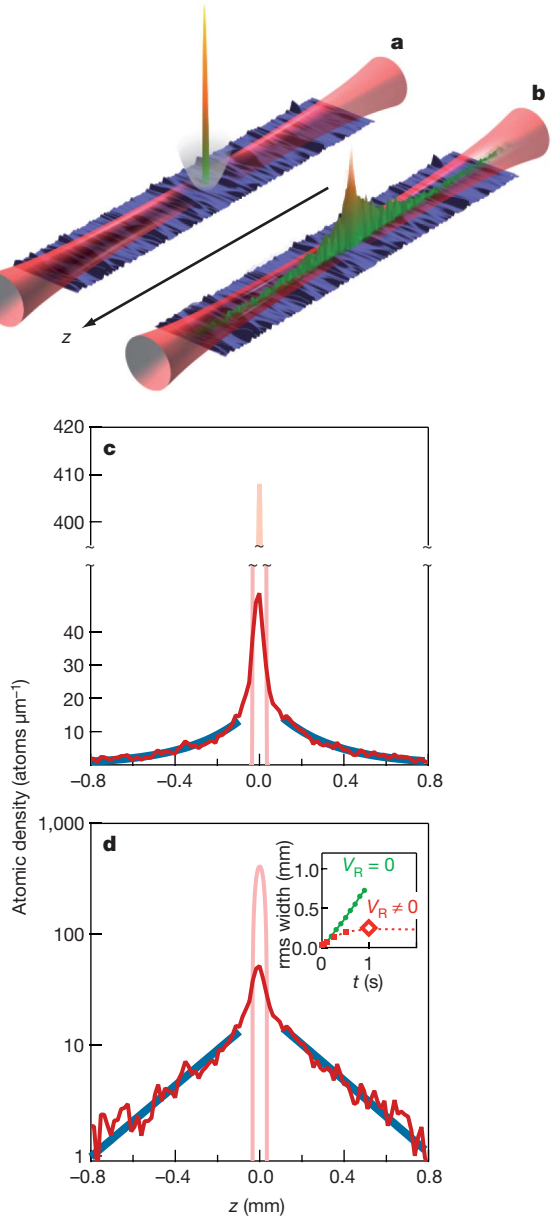

Figure 1 | Observation of exponential localization. **a**, A small BEC (1.7×10^4 atoms) is formed in a hybrid trap that is the combination of a horizontal optical waveguide, ensuring a strong transverse confinement, and a loose magnetic longitudinal trap. A weak disordered optical potential, transversely invariant over the atomic cloud, is superimposed (disorder amplitude V_R low in comparison with the chemical potential μ_{in} of the initial BEC). **b**, When the longitudinal trap is switched off, the BEC starts expanding and then localizes, as observed by direct imaging of the fluorescence of the atoms irradiated by a resonant probe. In **a** and **b**, false-colour images and sketched profiles are for illustration purposes; they are not exactly to scale. **c**, **d**, Density profiles (red) of the localized BEC one second after release, in linear (**c**) and semi-log (**d**) coordinates. In the inset in **d** we display the root-mean-square (rms) width of the profile versus time t, with ($V_R \neq 0$) and without ($V_R = 0$) disordered potential. This shows that the stationary regime is reached after 0.5 s. The diamond at $t = 1$ s corresponds to the data shown in **c** and the main panel of **d**. Blue lines in **c** are exponential fits to the wings, and correspond to the straight blue lines in **d**. The narrow central profiles (pink) represent the trapped condensate before release ($t = 0$ s).

Transversely, the correlation function (an ellipse with semi-axis lengths of 97 μm and 10 μm) is much wider than the atomic matter wave, and we can therefore consider the disorder as being one-dimensional for the BEC expanding along the z direction. Along this direction, the correlation function of the disordered potential is $V_R^2(\sin(z/\sigma_R)/(z/\sigma_R))^2$, where the correlation length $\sigma_R = 0.26 \pm 0.03$ μm (±1 s.e.m.) is calculated knowing the numerical aperture of the optics, and V_R is the amplitude of the disorder. The corresponding speckle grain size is $\pi\sigma_R = 0.82$ μm. The power spectrum of this speckle potential is non-zero only for **k**-vectors lower in magnitude than a cutoff of $2/\sigma_R$. The amplitude of the disorder is directly proportional to the laser intensity[22]. The calibration factor is calculated knowing the geometry of the optical system and the properties of the rubidium-87 atoms.

When we switch off the longitudinal trapping in the presence of weak disorder, the BEC starts expanding, but the expansion rapidly stops, in stark contrast with the free expansion case (Fig. 1d inset, showing the evolution of the root-mean-square width of the observed profiles). Plots of the density profile in linear (Fig. 1c) and semi-log (Fig. 1d) coordinates then show clear exponential wings, a signature of Anderson localization. Our observations are made in a regime allowing Anderson localization, unlike in the experiments in refs 19 and 20. First, the disorder is weak enough ($V_R/\mu_{in} = 0.12$) that the initial interaction energy per atom is rapidly converted into a kinetic energy of the order of μ_{in} for atoms in the wings. This value is much greater than the amplitude of the disordered potential, so there is no possibility of a classical reflection from a potential barrier. Second, the atomic density in the wings is low enough (two orders of magnitude less than in the initial BEC) that the interaction energy is negligible in comparison with the atom kinetic energy. Last, we fulfil the criterion, emphasized in ref. 13, that the atomic matter wave **k**-vector distribution be bounded, with a maximum magnitude k_{max} of less than half the cutoff in the power spectrum of the speckle disordered potential used here, that is, $k_{max}\sigma_R < 1$. The value of k_{max} is measured directly by observing the free expansion of the BEC in the waveguide in the absence of disorder (see Methods). For the runs corresponding to Figs 1c, 1d, 2, and 3, we have $k_{max}\sigma_R = 0.65 \pm 0.09$ (±2 s.e.m.).

An exponential fit to the wings of the density profiles yields the localization length L_{loc}, which we can compare to the theoretical value[13]

$$L_{loc} = \frac{2\hbar^4 k_{max}^2}{\pi m^2 V_R^2 \sigma_R (1 - k_{max}\sigma_R)} \quad (1)$$

valid only for $k_{max}\sigma_R < 1$ (m is the atomic mass). To ensure that the comparison is meaningful, we first check that we have reached a stationary situation, in which the fitted value of L_{loc} no longer evolves, as shown in Fig. 2. In Fig. 3, we plot the variation of L_{loc} with the disorder amplitude V_R, for the same number of atoms, that is, the same k_{max}. The dash–dot line is a plot of equation (1) for the values of k_{max} and σ_R determined as explained above. It shows quite a good agreement between our measurements and the theoretical predictions: with no adjustable parameters we obtain the correct magnitude and general shape. The shaded area reflects the envelope of the dash–dot line when we take into account the uncertainties in σ_R and k_{max}. The uncertainty in the calibration of V_R does not appear in Fig. 3. We estimate it to be no greater than 30%, which does not affect the agreement between theory and experiment.

An intriguing result of ref. 13 is the prediction of density profiles with algebraic wings when $k_{max}\sigma_R > 1$, that is, when the initial interaction energy is great enough that a fraction of the atoms have a **k**-vector greater in magnitude than $1/\sigma_R$, which plays the role of an effective mobility edge. We investigate this regime by repeating the experiment with a BEC containing more atoms (1.7×10^5 atoms, $\mu_{in}/h = 519$ Hz), for $V_R/\mu_{in} = 0.15$. Figure 4a shows the observed density profile in such a situation ($k_{max}\sigma_R = 1.16 \pm 0.14$ (±2 s.e.m.)), and a log–log plot suggests a power-law decrease in the wings, with an

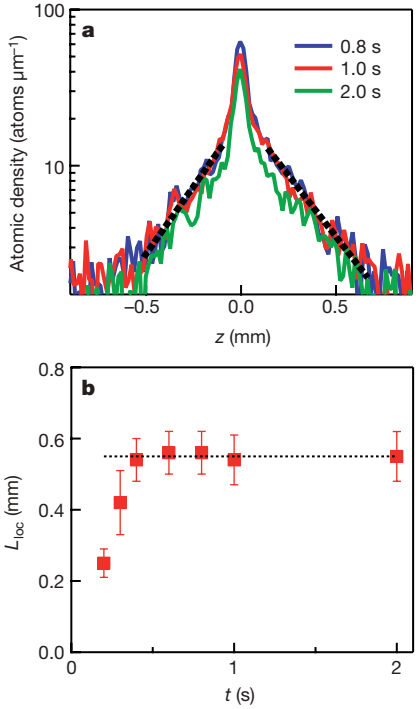

Figure 2 | Stationarity of the localized profile. **a**, Three successive density profiles, from which the localization length L_{loc} is extracted by fitting an exponential, $\exp(-2|z|/L_{loc})$ (dotted black lines), to the atomic density in the wings. **b**, Localization length L_{loc} versus expansion time t. Error bars, 95% confidence intervals for the fitted values (± 2 s.e.m.).

exponent of 1.95 ± 0.10 (± 2 s.e.m.), in agreement with the theoretical prediction that density decreases like $1/z^2$ in the wings. The semi-log plot (inset) confirms that an exponential would not work as well. For comparison, we present in Fig. 4b a log–log plot and a semi-log plot (inset) for the case with $k_{max}\sigma_R = 0.65$ and $V_R/\mu_{in} = 0.15$, where we conclude in favour of exponential rather than algebraic tails. These data support the existence of a crossover from an exponential to an algebraic regime in our speckle potential.

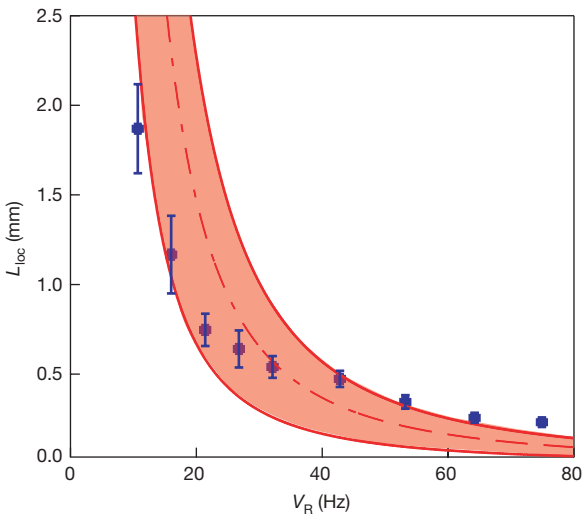

Figure 3 | Localization length versus amplitude of the disordered potential. L_{loc} is obtained by an exponential fit to the wings of the stationary localized density profiles, as shown in Fig. 2. Error bars, 95% confidence intervals for the fitted values (± 2 s.e.m.); 1.7×10^4 atoms ; $\mu_{in} = 219$ Hz. The dash–dot line is plotted using equation (1), where k_{max} is determined from the observed free expansion of the condensate (see Methods). The shaded area represents uncertainty associated with the evaluations of k_{max} and σ_R. We note that the limited extension of the disordered potential (4 mm) allows us to measure values of L_{loc} up to about 2 mm.

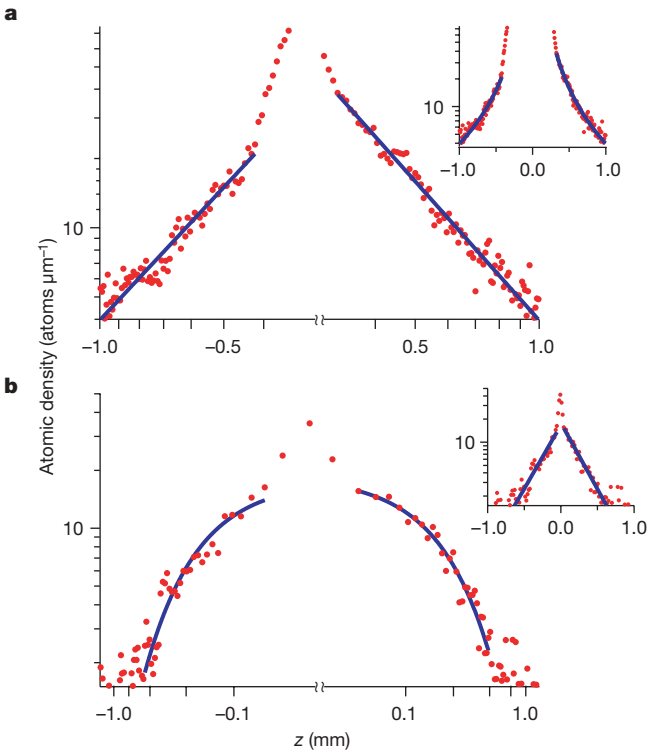

Figure 4 | Algebraic and exponential regimes in a one-dimensional speckle potential. Log–log and semi-log plots of the stationary atomic density profiles, showing the difference between the algebraic ($k_{max}\sigma_R > 1$) and exponential ($k_{max}\sigma_R < 1$) regimes. **a**, Density profile for $V_R/\mu_{in} = 0.15$ and $k_{max}\sigma_R = 1.16 \pm 0.14$ (± 2 s.e.m.). The momentum distribution of the released BEC has components beyond the effective mobility edge $1/\sigma_R$. The fit to the wings with a power-law decay $1/|z|^\beta$ yields $\beta = 1.92 \pm 0.06$ (± 2 s.e.m.) for the left-hand wing and $\beta = 2.01 \pm 0.03$ (± 2 s.e.m.) for the right-hand wing. The inset shows the same data in a semi-log plot, and confirms the non-exponential decay. **b**, For comparison, a similar set of plots (log–log and semi-log) in the exponential regime for the same $V_R/\mu_{in} = 0.15$ and $k_{max}\sigma_R = 0.65 \pm 0.09$ (± 2 s.e.m.).

Direct imaging of atomic quantum gases in controlled, optical disordered potentials is a promising technique to investigate a variety of open questions on disordered quantum systems. First, as in other problems of condensed matter simulated using ultracold atoms, direct imaging of atomic matter waves offers unprecedented possibilities to measure important properties, such as localization lengths. Second, our experiment can be extended to quantum gases with controlled interactions where localization of quasi-particles[26,27], Bose glass[14,15,28] and Lifshits glass[29] are expected, as well as to Fermi gases and to Bose–Fermi mixtures where rich phase diagrams have been predicted[30]. The reasonable quantitative agreement between our measurements and the theory of one-dimensional Anderson localization in a speckle potential demonstrates the high degree of control in our set-up. We thus anticipate that it can be used as a quantum simulator for investigating Anderson localization in higher dimensions[31,32], first to look for the mobility edge of the Anderson transition, and then to measure important features at the Anderson transition that are still under theoretical investigation, such as critical exponents. It will also become possible to investigate the effect of controlled interactions on Anderson localization.

METHODS SUMMARY

Momentum distribution of the expanding BEC. To compare measured localization lengths with those calculated from equation (1), we need to know k_{max}, the maximum amplitude of the **k**-vector distribution of the atoms, at the beginning of the expansion in the disordered potential. We measure k_{max} by releasing a BEC with the same number of atoms in the waveguide without disorder, and observing the density profiles at various times t. Density profiles are readily

converted into **k**-vector distributions ($|\mathbf{k}| = \hbar^{-1} m \mathrm{d}z/\mathrm{d}t$). The key step in obtaining $k_{\max}$ is accurately determining the position $z_{\max}$ of the front edge of the profile. To do this, we fit the whole profile to an inverted parabola, which is the expected shape for the one-dimensional expansion of a BEC in the fundamental transverse mode of the waveguide. Actually, the BEC has an initial transverse profile that is slightly enlarged owing to interactions between atoms, but its density rapidly decreases during the expansion, and a numerical calculation using our experimental parameters shows that for expansion times greater than $t = 0.2$ s, an inverted parabola correctly approximates the atomic density profile and allows accurate determination of the front edge position. Using this procedure, we measure $z_{\max}$ every 0.1 s from $t = 0$ to $t = 1$ s, and find it to be proportional to t for $t > 0.2$ s. We estimate the uncertainty in $k_{\max}$ to about 6% and 9% for 1.7×10^5 atoms and 1.7×10^4 atoms, respectively.

Received 14 March; accepted 9 April 2008.

1. Anderson, P. W. Absence of diffusion in certain random lattices. *Phys. Rev.* **109,** 1492–1505 (1958).
2. Van Tiggelen, B. in *Wave Diffusion in Complex Media 1998* (ed. Fouque, J. P.) 1–60 (Kluwer, Dordrecht, 1999).
3. Wiersma, D. S., Bartolini, P., Lagendijk, A. & Righini, R. Localization of light in a disordered medium. *Nature* **390,** 671–673 (1997).
4. Scheffold, F., Lenke, R., Tweer, R. & Maret, G. Localization or classical diffusion of light? *Nature* **398,** 206–270 (1999).
5. Störzer, M., Gross, P., Aegerter, C. M. & Maret, G. Observation of the critical regime near Anderson localization of light. *Phys. Rev. Lett.* **96,** 063904 (2006).
6. Schwartz, T., Bartal, G., Fishman, S. & Segev, M. Transport and Anderson localization in disordered two-dimensional photonic lattices. *Nature* **446,** 52–55 (2007).
7. Lahini, Y. *et al.* Anderson localization and nonlinearity in one-dimensional disordered photonic lattices. *Phys. Rev. Lett.* **100,** 013906 (2008).
8. Dalichaouch, R., Armstrong, J. P., Schultz, S., Platzman, P. M. & McCall, S. L. Microwave localization by two-dimensional random scattering. *Nature* **354,** 53–55 (1991).
9. Chabanov, A. A., Stoytchev, M. & Genack, A. Z. Statistical signatures of photon localization. *Nature* **404,** 850–853 (2000).
10. Weaver, R. L. Anderson localization of ultrasound. *Wave Motion* **12,** 129–142 (1990).
11. Akkermans, E. & Montambaux, G. *Mesoscopic Physics of Electrons and Photons* (Cambridge Univ. Press, Cambridge, UK, 2006).
12. Goodman, J. W. *Speckle Phenomena in Optic*s (Roberts, Greenwood Village, Colorado, 2007).
13. Sanchez-Palencia, L. *et al.* Anderson localization of expanding Bose-Einstein condensates in random potentials. *Phys. Rev. Lett.* **98,** 210401 (2007).
14. Giamarchi, T. & Schulz, H. J. Anderson localization and interactions in one-dimensional metals. *Phys. Rev. B* **37,** 325–340 (1988).
15. Fisher, M. P. A., Weichman, P. B., Grinstein, G. & Fisher, D. S. Boson localization and the superfluid-insulator transition. *Phys. Rev. B* **40,** 546–570 (1989).
16. Bloch, I., Dalibard, J. & Zwerger, W. Many-body physics with ultracold atoms. *Rev. Mod. Phys.* (in the press); preprint at ⟨http://arxiv.org/abs/0704.3011⟩ (2007).
17. Lewenstein, M. *et al.* Ultracold atomic gases in optical lattices: mimicking condensed matter physics and beyond. *Adv. Phys.* **56,** 243–379 (2007).
18. Damski, B., Zakrzewski, J., Santos, L., Zoller, P. & Lewenstein, M. Atomic Bose and Anderson glasses in optical lattices. *Phys. Rev. Lett.* **91,** 080403 (2003).
19. Clément, D. *et al.* Suppression of transport of an interacting elongated Bose–Einstein condensate in a random potential. *Phys. Rev. Lett.* **95,** 170409 (2005).
20. Fort, C. *et al.* Effect of optical disorder and single defects on the expansion of a Bose–Einstein condensate in a one-dimensional waveguide. *Phys. Rev. Lett.* **95,** 170410 (2005).
21. Schulte, T. *et al.* Routes towards Anderson-like localization of Bose–Einstein condensates in disordered optical lattices. *Phys. Rev. Lett.* **95,** 170411 (2005).
22. Clément, D. *et al.* Experimental study of the transport of coherent interacting matter-waves in a 1D random potential induced by laser speckle. *N. J. Phys.* **8,** 165, doi:10.1088/1367-2630/8/8/165 (2006).
23. Moore, J. L., Robinson, J. C., Bharucha, C., Williams, P. E. & Raizen, M. G. Observation of dynamical localization in atomic momentum transfer: A new testing ground for quantum chaos. *Phys. Rev. Lett.* **73,** 2974–2977 (1994).
24. Chabé, J. *et al.* Experimental observation of the Anderson transition with atomic matter waves. Preprint available at ⟨http://arxiv.org/abs/0709.4320⟩ (2007).
25. Guerin, W. *et al.* Guided quasicontinuous atom laser. *Phys. Rev. Lett.* **97,** 200402 (2006).
26. Bilas, N. & Pavloff, N. Anderson localization of elementary excitations in a one-dimensional Bose–Einstein condensate. *Eur. Phys. J. D* **40,** 387–397 (2006).
27. Lugan, P., Clément, D., Bouyer, P., Aspect, A. & Sanchez-Palencia, L. Anderson localization of Bogolyubov quasiparticles in interacting Bose–Einstein condensates. *Phys. Rev. Lett.* **99,** 180402 (2007).
28. Fallani, L., Lye, J. E., Guarrera, V., Fort, C. & Inguscio, M. Ultracold atoms in a disordered crystal of light: towards a Bose glass. *Phys. Rev. Lett.* **98,** 130404 (2007).
29. Lugan, P. *et al.* Ultracold Bose gases in 1D-disorder: from Lifshits glass to Bose–Einstein condensate. *Phys. Rev. Lett.* **98,** 170403 (2007).
30. Sanpera, A., Kantian, A., Sanchez-Palencia, L., Zakrzewski, J. & Lewenstein, M. Atomic Fermi–Bose mixtures in inhomogeneous and random optical lattices: from Fermi glass to quantum spin glass and quantum percolation. *Phys. Rev. Lett.* **93,** 040401 (2004).
31. Kuhn, R. C., Miniatura, C., Delande, D., Sigwarth, O. & Müller, C. A. Localization of matter waves in two-dimensional disordered optical potentials. *Phys. Rev. Lett.* **95,** 250403 (2005).
32. Skipetrov, S. E., Minguzzi, A., van Tiggelen, B. A. & Shapiro, B. Anderson localization of a Bose-Einstein condensate in a 3D random potential. *Phys. Rev. Lett.* **100,** 165301 (2008).

Acknowledgements: The authors are indebted to P. Chavel, T. Giamarchi, M. Lewenstein and G. Shlyapnikov for many discussions, to P. Georges and G. Roger for assistance with the laser, and to F. Moron, A. Villing and G. Colas for technical assistance on the experimental apparatus. This research was supported by the Centre National de la Recherche Scientifique (CNRS), the Délégation Générale de l'Armement (DGA), the Ministère de l'Education Nationale, de la Recherche et de la Technologie (MENRT), the Agence Nationale de la Recherche (ANR), the Institut Francilien de Recherche sur les Atomes Froids (IFRAF) and IXSEA; by the STREP programme FINAQS of the European Union; and by the programme QUDEDIS of the European Science Foundation (ESF).

Author Information Reprints and permissions information is available at www.nature.com/reprints. Correspondence and requests for materials should be addressed to P.B. (philippe.bouyer@institutoptique.fr).